Finite Element Simulation of an Out-of-Phase Synchronization of a Synchronous Machine

Silvio Ikuyo Nabeta
Equipe de Simulação de Fenômenos Eletromagnéticos - Depto. de Engenharia de Energia e Automação Elétricas
Escola Politécnica da Universidade de São Paulo
Av. Prof. Luciano Gualberto trav. 3 nº 158 Cidade Universitária CEP 05508-900 São Paulo, Brazil

Albert Foggia, Jean-Louis Coulomb, Gilbert Reyne
Laboratoire d'Electrotechnique de Grenoble (INPG) URA CNRS 355
BP 46, 38402 Saint-Martin d'Hères Cedex, France

***Abstract*—This paper presents the finite element simulations of the out-of-phase synchronization of a synchronous machine with an external electric system. Two cases were analysed regarding to the phase angle: 120° and 180°. Computed results are analysed and compared to analytical values.**

INTRODUCTION

A very current and important stress for a synchronous machine arises during an out-of-phase synchronization.

An out-of-phase synchronization is a faulty three phase operation that occurs when the generator is switched to the system and the equality of voltage and/or frequency and/or phase are not respected.

In this work we assume that the voltage is equal for the system and the generator, and the phase angle is different.

Fig.1 shows the representation of this assumption.

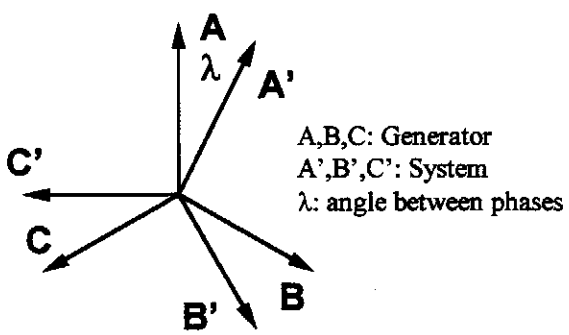

Fig.1: Angle lag between generator and system voltages

In such condition two important cases arise:

1. out-of-phase synchronization with 180° of angular lag;
2. out-of-phase synchronization with 120° of angular lag.

In the first case the armature currents reach the maximum value whereas in the second case the electromagnetic torque reaches its maximum value.

The analytical study of those cases is done by the Park theory [1].

Nevertheless, the equations development is very fastidious and some simplifying hypothesis must be taken in order to obtain useful expressions.

Nowadays, the availability of modern numerical programs allows a closer investigation of the magnetic behaviour in the synchronous machine.

Hence a more accurate solution can be reached by computing the flux distributions in detail avoiding simplifications in modelling.

This paper presents the linear, two-dimensional , time-stepping finite element simulations of the out-of-phase synchronization in the two cases previously mentioned.

These simulations considered the rotor movement by means of the air-band technique [5] and the external system by coupling electric circuit equations to the Finite Element Method (FEM) [2], [3], [4].

Computed results are compared to analytical ones.

OUT-OF-PHASE SYNCHRONIZATION - THEORETICAL OVERVIEW

Consider a unloaded synchronous generator. The armature voltages can be written as:

$$\begin{aligned} V_{a0} &= e.sin(\omega t + \theta_0) \\ V_{b0} &= e.sin\left(\omega t + \theta_0 - \frac{2\pi}{3}\right) \\ V_{c0} &= e.sin\left(\omega t + \theta_0 - \frac{4\pi}{3}\right) \end{aligned} \quad (1)$$

As stated before only the phase equality is not respected.

Thus the system voltages are expressed as:

$$\begin{aligned} V_{a1} &= e.sin(\omega t + \theta_0 - \lambda) \\ V_{b0} &= e.sin\left(\omega t + \theta_0 - \lambda - \frac{2\pi}{3}\right) \\ V_{c0} &= e.sin\left(\omega t + \theta_0 - \lambda - \frac{4\pi}{3}\right) \end{aligned} \qquad (2)$$

where λ is the phase angle difference at the switching instant.

Applying the Park transformation to (1) and (2) we obtain:

$$V_{d0} = 0 \qquad V_{d1} = -e.sin\lambda$$
$$V_{q0} = e \qquad V_{q1} = e.\cos\lambda$$

The voltage variation on the machine's terminal is:

$$\begin{aligned} \Delta V_{d0} &= V_{d1} - V_{d0} = -e.sin\lambda = -2e.sin\frac{\lambda}{2}.\cos\frac{\lambda}{2} \\ \Delta V_{q0} &= V_{q1} - V_{q0} = e.\cos\lambda - e = -2e.sin^2\frac{\lambda}{2} \end{aligned} \qquad (3)$$

Using the operational notation we have:

$$\begin{aligned} \frac{\Delta V_{d0}}{p} &= -p\Delta\phi_d - \omega.\Delta\phi_q - r_a.\Delta I_d \\ \frac{\Delta V_{q0}}{p} &= -p\Delta\phi_q + \omega.\Delta\phi_d - r_a.\Delta I_q \end{aligned} \qquad (4)$$

with:

$$\begin{aligned} \Delta\phi_d &= L_d(p).\Delta I_d \\ \Delta\phi_q &= L_q(p).\Delta I_q \end{aligned} \qquad (5)$$

$L_d(p)$: D-axis operational inductance

$L_q(p)$: Q-axis operational inductance

Eliminating ΔI_d and ΔI_q in equations (4) we reach the following system:

$$\begin{bmatrix} \frac{\Delta V_{d0}}{p} \\ \frac{\Delta V_{q0}}{p} \end{bmatrix} = \begin{bmatrix} -\left(p + \frac{r_a}{L_d(p)}\right) & -\omega \\ \omega & -\left(p + \frac{r_a}{L_q(p)}\right) \end{bmatrix} \begin{bmatrix} \Delta\phi_d \\ \Delta\phi_q \end{bmatrix} \qquad (6)$$

Solving (6) we obtain:

$$\Delta\phi_d(p) = \frac{1}{p\left(p^2 + 2\alpha p + \omega^2\right)} \times \left[-\Delta V_{d0}.\left(p + \frac{r_a}{L_d(p)}\right) + \Delta V_{q0}.\omega\right] \qquad (7)$$

$$\Delta\phi_q(p) = \frac{1}{p\left(p^2 + 2\alpha p + \omega^2\right)} \times \left[-\Delta V_{d0}.\omega - \Delta V_{q0}.\left(p + \frac{r_a}{Lq(p)}\right)\right]$$

where: $\frac{1}{\alpha} = T_a$ is the armature time-constant

Considering that the out-of-phase operation is harmful in the first instants we can neglect all resistances.

So, introducing (7) in equation (5) we obtain the currents variations:

$$\Delta I_d(p) = \frac{\Delta V_{d0}}{L_d(p)\left(p^2 + 2\alpha p + \omega^2\right)} + \frac{\omega.\Delta V_{q0}}{pL_d(p)\left(p^2 + 2\alpha p + \omega^2\right)} \qquad (8)$$

$$\Delta I_q(p) = \frac{\Delta V_{d0}}{pL_q(p)\left(p^2 + 2\alpha p + \omega^2\right)} + \frac{\omega.\Delta V_{q0}}{L_q(p)\left(p^2 + 2\alpha p + \omega^2\right)}$$

Moreover, assuming that $X_d^{"} = X_q^{"}$ we obtain in the time-domain terms [1]:

$$I_d(t) = \Delta I_d(t) = \frac{2e}{X_d^{"}}.\sin\frac{\lambda}{2}\left[\sin\left(\omega t + \frac{\lambda}{2}\right) - \sin\frac{\lambda}{2}\right]$$

$$I_q(t) = \Delta I_q(t) = -\frac{2e}{X_d^{"}}.\sin\frac{\lambda}{2}\left[\cos\left(\omega t + \frac{\lambda}{2}\right) - \cos\frac{\lambda}{2}\right] \quad (9)$$

and: $X_d^{"}$: D-axis subtransient reactance

And the phase-A current can be written, in per unit values, as:

$$I_a(t) = \frac{2e}{X_d^{"}}.\sin\frac{\lambda}{2}\left[\sin\left(\omega t - \theta_0 - \frac{\lambda}{2}\right) - \sin\left(\theta_0 - \frac{\lambda}{2}\right)\right] \quad (10)$$

The torque equation is obtained by using the following equation:

$$C_e = \frac{e^2}{X_d^{"}}.\omega\left[\phi_d.I_q - \phi_q.I_d\right] \quad (11)$$

In our case we have in per unit values:

$$C_e = \frac{e^2}{X_d^{"}}\left[\sin\lambda - 2\sin\frac{\lambda}{2}.\cos\left(\omega t + \frac{\lambda}{2}\right)\right] \quad (12)$$

It can be noted from (10) that the maximum current occurs when:

$$\lambda = \pi, \theta_0 = 0, \omega t = \pi$$

Thus:

$$I_{amax} = \frac{4e}{X_d^{"}} \quad (13)$$

Analogously, from (12) we have for the maximum torque:

$$\lambda = \pm\frac{2\pi}{3}$$

and:

$$C_{emax} = \frac{3\sqrt{3}.e^2}{2X_d^{"}} \quad (14)$$

FINITE ELEMENT METHOD

Although analytical solutions are known for the out-of-phase synchronization as presented in the previous section numerical methods have the advantage of providing solutions less affected by simplifications including results on local quantities.

This section presents the FEM for time-dependent problems.

In electromagnetic time-dependent problems the skin effect occurs in solid conductors.

Thus the partial differential equations that describe the electromagnetic phenomenon are:

for wound conductors:

$$rot(\nu.rotA) = j \quad (15)$$

for solid conductors:

$$\text{rot}(\nu.rotA) + \sigma.(\partial A/\partial t + gradV) = 0 \quad (16)$$

Applying the FEM to these equations the following systems, in commonly used notations, are reached [2]:

wound conductors:

$$[S].[A] = [C].[I] \quad (17)$$

solid conductors:

$$[S].[A] + [G].\partial[A]/\partial t.[C'].[\Delta V] \quad (18)$$

with:

$$S_{i,j} = l.\iint_{\Omega} \nu.grad\alpha_i.grad\alpha_j d\Omega$$

$$G_{i,j} = l.\iint_{\Omega} \sigma.\alpha_i.\alpha_j d\Omega$$

$$C_i' = l.\iint_{\Omega_k} \sigma.\alpha_i d\Omega$$

$$C_i = \left(\frac{N_s.l}{s_k}\right)\iint_{\Omega_k} \alpha_i d\Omega$$

α_i, α_j :interpolation functions
N_s : number of turns for wound conductors
s_k : wound conductors' region surface

It is noted that wound conductors are supplied by current sources whereas the most electromechanical devices are supplied by voltage sources.

Therefore, a technique, as shown in the following section, is necessary to take into account the two types of conductors and to allow the voltage supply in wound conductors.

Electric Circuits Coupling

A recently developed technique to model wound and solid conductors and the voltage supply is the Electric Circuits Coupling which is based on the association of Kirchhoff equations in the FEM formulations [2].

Furthermore, it allows to take into account the external components such as inductances and resistances in the analysis.

Fig.2. shows a simplified circuit coupled with a Finite Element analysis.

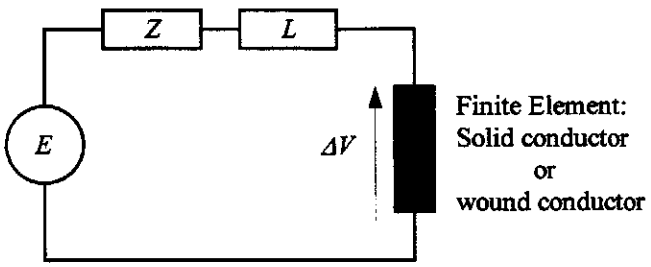

Fig.2. Electric Circuit Coupling

According to [2] the circuit coupling provides the following system:

for wound conductors:

$$[S].[A] = [C].[I] \quad (19)$$

$$[E] = [Z'].[I] + [L].\partial[I]/\partial t + [D'].[C'].\partial[A]/\partial t \quad (20)$$

for solid conductors:

$$[S].[A] + [G].\partial[A]/\partial t - [C'].[\Delta V] = 0 \quad (21)$$

$$[E] = [Z].[I] + [L].\partial[I]/\partial t + [D].[\Delta V] \quad (22)$$

$$[\Delta V] = [R].[I] + [R].[C]^{T}.\partial[A]/\partial t \quad (23)$$

where:

$[E]$:vector of voltage sources

$[A]$:vector of magnetic potentials

$[Z]$:matrix of external resistances

$[Z']$:matrix of external and wound conductors resistances

$[L]$:matrix of external inductances

$[D']$, $[D]$:matrices of currents directions

$[I]$:vector of currents

$[R]$:matrix of solid conductors resistances

$[\Delta V]$:vector of solid conductors drop voltages

Moving-Air-Band Technique

The moving-air-band technique was implemented in order to consider the rotor movement in the FEM simulation [5].

It comprises a surface located in the air-gap with only one layer of elements.

The main advantage of this technique is the fact that the finite element meshes in the stator and rotor remain unaltered after the movement.

Remeshing is necessary only in the band region as can be seen in Fig.3.

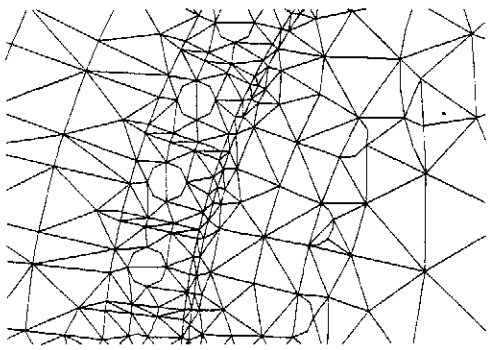

a: before

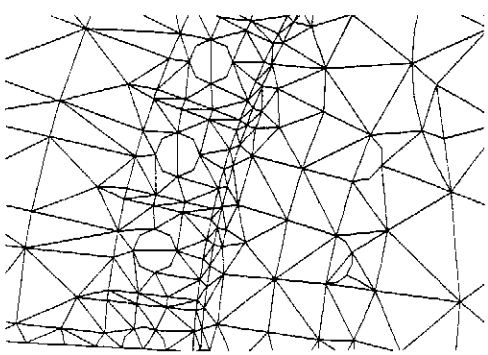

b: after

Fig.3. Moving-air-band mesh before and after a rotation of 5°

NUMERICAL SIMULATION

The numerical simulations were carried out on a 3-phase, 3 KVA, 50 Hz, 4 salient-pole generator, as shown in Fig.4.

The stator has 54 slots, 12 conductors per slot and a 2-tier, double-layer, star-connected winding.

The rotor, which is completely laminated, has 4-coil main excitation winding and a concentric wound damper winding fitted in 24 slots with 74 conductors per slot.

Figure 5 shows a magnified view of damper slots.

Due to symmetries in the study domain a half geometry was used in numerical analysis.

This allowed to reduce the matrices dimensions and the number of electric circuits.

The external system, the switches and the windings connections were taken into account in the simulations by using the electric circuit shown in Fig.6.

The software package used was FLUX2D [6].

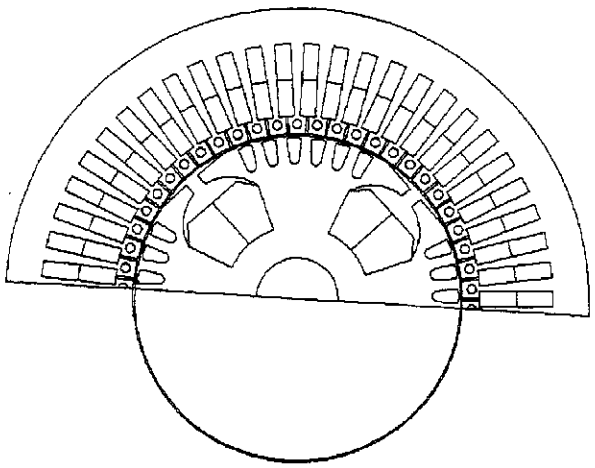

Fig.4. Machine geometry with moving-air-band technique

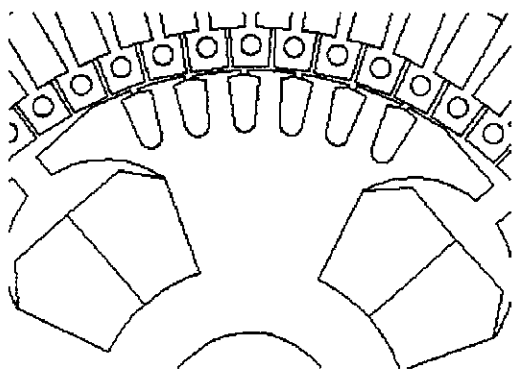

Fig.5. Magnified view of damper slots

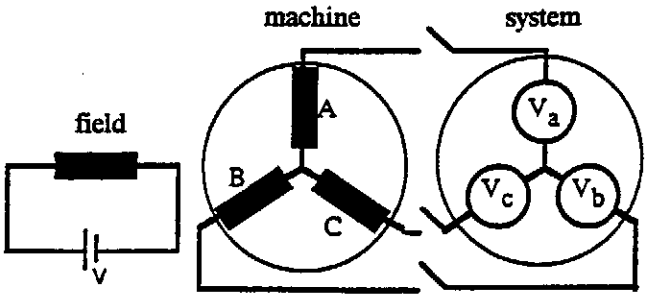

Fig.6. Electric circuit

The first step of the simulation consisted in reaching the generator steady-state at unload condition.

It was done by a time-stepping simulation feeding the field winding with a DC voltage source and rotating the rotor at 1500 rpm.

Afterwards, switching with the appropriate angle the out-of-phase synchronization between the generator and the system was accomplished.

In this work the time-step was 0.5 ms and synchronizing angles were chosen as $\lambda = 180°$ and $\lambda = 120°$.

RESULTS

Fig.7. shows the phase-A current and the torque waveforms for the out-of-phase synchronizations at 120° and 180°.

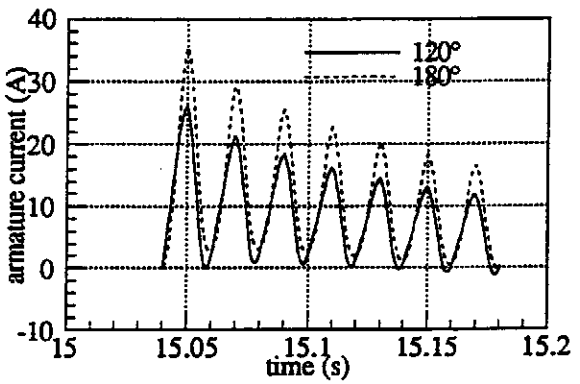

a: Current

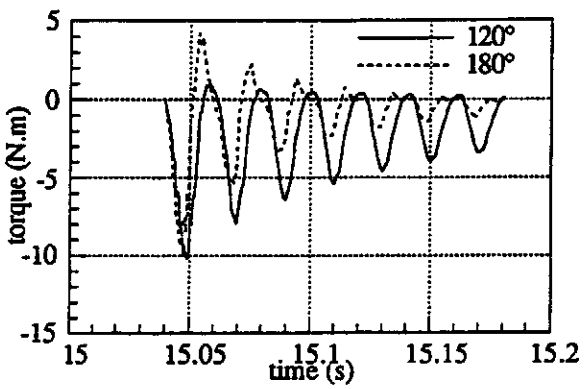

b: Torque

Fig.7. Phase-A current and torque for λ=120° and λ=180°

Table I presents the comparison between computed and analytical results of maxima values of current and torque.

Table I: Maxima values of current and torque

Method	Parameter	I_{max} (A) $\lambda=180°$	C_{max} (N.m) $\lambda=120°$
Analytical		40,3	-8,07
Simulation		35,5	-10,20

We note from Table I that for $\lambda=180°$ the analytical value for the current is greater than the simulated result.

This difference can be explained by the fact that all resistances in the analytical expressions were neglected.

Indeed, neglecting the resistances the decrements in the current waveform are not taken into account.

Furthermore, the absence of the resistances causes the non-consideration of the homopolar torque which can justify the difference between analytical and numerical results for the torque at $\lambda=120°$.

The total cpu time was 84.10^4 s and the number of unknowns was 5383.

CONCLUSIONS

Out-of-phase synchronizations between a synchronous generator and an external system were accomplished by finite element simulations.

Numerical results agree with theory and have shown that maximum current and maximum torque occur at $\lambda=180°$ and $\lambda=120°$, respectively.

Moreover, unlike analytical method, numerical simulations allow the out-of-phase synchronization study without neglecting the resistances.

Hence, complex phenomena such as the homopolar torque are taken into account and more complete results are reached.

AKNOWLEDGMENTS

The authors aknowledge the CNPq - National Council for Scientific and Technological Development for the financial support during this work.

REFERENCES

[1] P. Barret, *Régimes Transitoires des Machines Tournantes Electriques*, Editions Eyrolles, Paris, (1982).

[2] P. Lombard, G. Meunier, A general purpose method for electric and magnetic combined problems for 2D, axisymmetric and transients systems, *CEFC 92*, 3-5 aug, Claremont, USA. *IEEE Transactions on Magnetics*, vol.29, n.2, pp.1737-1740, March 1993.

[3] A. Arkkio, Finite Element Analysis of Cage Induction Motors fed by Static Frequency Converters, *IEEE Transactions on Magnetics*, vol.26, n.2, pp.551-554, 1990.

[4] N. Sadowski, B. Carly, Y. Lefèvre, M. Lajoie-Mazenc, Finite Element Simulation of Electrical Motors fed by Current Inverters, *IEEE Transactions on Magnetics*, vol.29, n.2, pp.1683-1688, March 1993.

[5] E. Vassent, G. Meunier, A. Foggia, G. Reyne, Simulation of induction machine operation using a step by step finite-element method coupled with circuit and mechanical equations, *Fifth joint MMM-Intermag Conf.* Pittsburgh, USA, 18-21 june, 1991. *IEEE Transactions on Magnetics*, vol.27, n.6, pp. 5232-5234, Nov. 1991.

[6] FLUX2D v.7.11 - Finite Element Software for Electromagnetics Applications, CEDRAT (CEE), MAGSOFT (USA).